

Reaction kinetics of muonium with the halogen gases (F₂, Cl₂, and Br₂)

Alicia C. Gonzalez, Ivan D. Reid,^{a)} David M. Garner, Masayoshi Senba, Donald G. Fleming,^{b)} Donald J. Arseneau, and James R. Kempton
 TRIUMF and Department of Chemistry, University of British Columbia, 4004 Wesbrook Mall, UBC Campus, Vancouver, British Columbia V6T 2A3, Canada

(Received 13 June 1989; accepted 1 August 1989)

Bimolecular rate constants for the thermal chemical reactions of muonium (Mu) with the halogen gases— $\text{Mu} + \text{X}_2 \rightarrow \text{MuX} + \text{X}$ —are reported over the temperature ranges from 500 down to 100, 160, and 200 K for $\text{X}_2 = \text{F}_2, \text{Cl}_2$, and Br_2 , respectively. The Arrhenius plots for both the chlorine and fluorine reactions show positive activation energies E_a over the whole temperature ranges studied, but which decrease to near zero at low temperature, indicative of the dominant role played by quantum tunneling of the ultralight muonium atom. In the case of $\text{Mu} + \text{F}_2$, the bimolecular rate constant $k(T)$ is essentially independent of temperature below 150 K, likely the first observation of Wigner threshold tunneling in gas phase (H atom) kinetics. A similar trend is seen in the $\text{Mu} + \text{Cl}_2$ reaction. The Br_2 data exhibit an apparent negative activation energy [$E_a = (-0.095 \pm 0.020) \text{ kcal mol}^{-1}$], constant over the temperature range of $\sim 200\text{--}400$ K, but which decreases at higher temperatures, indicative of a highly attractive potential energy surface. This result is consistent with the energy dependence in the reactive cross section found some years ago in the atomic beam data of Hepburn *et al.* [J. Chem. Phys. **69**, 4311 (1978)]. In comparing the present Mu data with the corresponding H atom kinetic data, it is found that Mu invariably reacts considerably faster than H at all temperatures, but particularly so at low temperatures in the cases of F_2 and Cl_2 . The current transition state calculations of Steckler, Garrett, and Truhlar [Hyperfine Interact. **32**, 779 (1986)] for $\text{Mu} + \text{X}_2$ account reasonably well for the rate constants for F_2 and Cl_2 near room temperature, but their calculated value for $\text{Mu} + \text{Br}_2$ is much too high. Moreover, these calculations seemingly fail to account for the trend in the $\text{Mu} + \text{F}_2$ and $\text{Mu} + \text{Cl}_2$ data toward pronounced quantum tunneling at low temperatures. It is noted that the Mu kinetics provide a crucial test of the accuracy of transition state treatments of tunneling on these early barrier HX_2 potential energy surfaces.

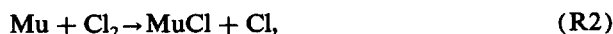
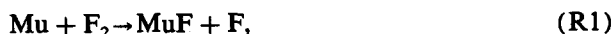
I. INTRODUCTION

It is well-known that the study of kinetic isotope effects for a given potential energy surface (PES) can provide important information about the dynamics of a chemical reaction on that surface. Here the remarkable mass ratio between the muonium ($\text{Mu} = \mu^+ + e^-$) and H atom isotopes [$m(\text{Mu}) \sim 1/9m(\text{H})$] can be very sensitive in elucidating the origin of dynamical effects on chemical reactivity.^{1–14} Both quantum tunneling^{4–14} and zero-point energy (ZPE) shifts at the transition state (TS)^{1–3,5,9,10,13–17} can be much more effectively tested by muonium than by any other hydrogen atom isotope. This has been demonstrated most recently in reports of the thermal reaction rates of Mu with H_2 and D_2 ,^{1–3,6–9} in which the three-dimensional (3D) quantum coupled states (3D QCS) calculations of Schatz^{6,7} on the chemically accurate Liu–Siegbahn PES for H_3 ^{18,19} gave exemplary agreement with experiment over the whole temperature range studied.^{1–3}

The reactions of H atoms with the halogen (X_2) gases has also received considerable attention over the years, brought into focus in the last decade or so by the development of chemical lasers.^{20,21} Like $\text{H} + \text{H}_2$, the reactions of $\text{H} + \text{X}_2$ are simple abstraction reactions, amenable to calcu-

lations by direct reaction theories. However, unlike the Liu–Siegbahn potential for H_3 , there are no similarly accurate *ab initio* surfaces for HX_2 .^{22–25} The study of isotopic mass effects on the reaction kinetics for $\text{H} + \text{X}_2$ plays a dual role. In addition to providing a test of reaction theory, the results are also important in helping to better define current semiempirical PES's for this system, which are predominately either of the London–Eyring–Polanyi–Sato (LEPS)^{26–33} or diatomics-in-molecules (DIM)^{34–37} variety, and will in turn ultimately improve the accuracy of *ab initio* calculations. In this endeavor, it is desirable to have as wide a variation in isotopic mass as possible, exemplified by the present study of $\text{Mu} + \text{X}_2$.

Experimental data available to date on rate constants for the gas phase thermal reactions

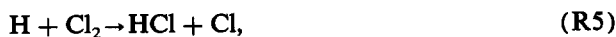


were obtained during the early stages of operation of the TRIUMF cyclotron by Garner, Fleming, and co-workers.^{5,38–41} Due to poor beam intensity at the time, these data are sparse, reported only for room temperature and above, and are characterized by relatively poor statistics. Reactions (R1)⁴⁰ and (R2)³⁹ have been reported at a few temperatures between 295 and 385 K, while there has been only one measurement of reaction (R3) reported, at 295

^{a)} Present address: Physikalisch–Chemisches Institut der Universität Zürich, Winterthurerstrasse 190, CH-8057 Zürich, Switzerland.

^{b)} 1989–89 Canada Council Killam Research Fellow.

K,³⁸ which has the distinction of being the first study of muonium reactivity in a low density gas (taken at the now defunct 184" cyclotron at Berkeley). Despite their importance to chemical lasers,²⁰ data on rate constants for the corresponding H atom reactions



are often determined from indirect measurements⁴²⁻⁴⁵ and are frequently in disagreement. The most recent direct measurement of $\text{H} + \text{F}_2$ by Homann *et al.*⁴⁶ using a flow system with mass spectrometric analysis over a wide temperature range, disagrees by a factor of 2 with the earlier results of Albright *et al.*,⁴⁷ also obtained by a flow system and mass spectrometric analysis and over a comparable temperature range. Of the two, the flow technique of Homann *et al.* should be the more reliable.⁴⁴ The rate constants for reaction (R5) have been measured directly by Wagner *et al.*,⁴⁸ using a flow system, but with detection of H atoms by Lyman- α fluorescence. Their results are in very good agreement with those of Bemand and Clyne,⁴⁹ obtained also by means of a resonance fluorescence technique over a range of temperatures, as well as with the more recent results of Jaffe and Clyne⁵⁰ at room temperature using the same fluorescence technique as in Ref. 49, but are in disagreement with those of Albright *et al.*,⁴⁷ Ambidge *et al.*,⁵¹ and Michael and Lee.⁵² The recommended results for reaction (R5)⁴⁵ are those of Wagner *et al.*⁴⁸ and Clyne and co-workers.^{49,50} As with reaction (R3), there has only been one direct room temperature measurement of reaction (R6) reported, by Jaffe and Clyne.⁵⁰ This agrees though with the indirect value reported by Malins and Setser⁴² relative to the measured value for reaction (R5).

Despite the relatively poor quality of the data reported by us earlier for reactions (R1)–(R3), they have been of considerable importance in comparisons with theoretical calculations of HX_2 reaction dynamics. The data for $\text{Mu} + \text{F}_2$ in particular were crucial in assessing the reliability of the early 1D quantum mechanical (1D QM) calculations of Connor and co-workers^{11,12} using a LEPS surface from the work of Jonathan *et al.*²⁸ Notable in these calculations was the good agreement obtained with the experimental Arrhenius activation energy for reaction (R1), which was almost a factor of 2 lower than that of its isotopic analog (R4). This was recognized at the time as being due to the importance of quantum tunneling in the case of $\text{Mu} + \text{F}_2$, even at temperatures above room temperature. Since then there have been additional PES's developed for HX_2 ^{25-27,31,34-37} as well as new theoretical calculations for H atom reaction kinetics on these surfaces. Several transition state theory (TST)^{10,13,14,53} and quasiclassical trajectory (QCT) calculations⁵³⁻⁵⁷ have been reported. In particular, the recent variational transition state theory (VTST) calculations of Steckler, Garrett, and Truhlar^{13,14} have utilized tunneling paths like those employed in similar calculations for $\text{Mu} + \text{H}_2(\text{D}_2)$,⁶⁻⁹ which proved to be quite accurate in comparison with the experimental data^{1,3} and with the "exact" 3D QMCS results of Schatz.^{6,7} All of these calculations

demonstrate the inherent importance of Mu reactivity to developing an understanding of the topography of the PES and of the reaction dynamics for HX_2 .

Accordingly, in order to provide a more complete data base for comparison between experiment and theory, we report herein new measurements of reactions (R1)–(R3) over the temperature range from ~ 500 K to well below room temperature, down to 100 K in the case of F_2 , complementing the earlier studies cited above. As in Ref. 1, our aim is to increase the range of experimental data to facilitate comparisons with available H atom data and with current theoretical calculations of Mu (H) atom reaction dynamics on the halogens. In particular, the tunneling paths used in the calculation of transmission coefficients in TST^{6-9,13,14} will be much more effectively tested by the current study of $\text{Mu} + \text{X}_2$ down to low temperatures than was the case for $\text{Mu} + \text{H}_2$, since the HX_2 surfaces have early barriers and hence tunneling is expected to dominate Mu reactivity.

II. EXPERIMENTAL

These experiments were conducted on the M20B and M15 "surface" muon channels at the TRIUMF cyclotron, a meson facility adjacent to the campus of the University of British Columbia. The details of the muon spin-rotation (μSR) experimental technique employed, particularly as applied to the study of muonium chemistry in gases, has been well described elsewhere^{5,41,58-60} and will only briefly be mentioned here. A beam of spin-polarized positive muons (μ^+) is stopped in the target of interest (in these experiments, ~ 1 atm Ar or N_2 with appropriate amounts of X_2). The target vessel is positioned between Helmholtz coils which provide a magnetic field transverse to the muon spin direction, causing the muon to precess with a characteristic Larmor frequency. The muon undergoes radioactive decay with a mean life of $2.2 \mu\text{s}$, producing a high energy positron that is ejected anisotropically, preferentially along the muon spin direction. The time evolution of the muon ensemble spin polarization appears as oscillations in the time differential histogram of the number of the decay positrons detected in a fixed direction, measured as a function of the survival time of the corresponding muons. In these experiments, two independent positron telescopes were employed, positioned on opposite sides of the target.

In an applied magnetic field of less than 10 G, the spin precession frequency of the muon in the paramagnetic Mu atom is 1.3 MHz G^{-1} , which is 103 times the precession frequency of a muon in a diamagnetic environment, such as a MuX molecule. Hence, the coherent precession of an ensemble of paramagnetic Mu atoms is exponentially damped as chemical reactions ($\text{Mu} + \text{X}_2$) place the muon into a diamagnetic environment (MuX) at randomly distributed times.^{41,61} In the present experiments, a magnetic field of 7.2 G was employed. The relaxation rate (λ) of the muonium precession signal is linearly related to the bimolecular rate constant k

$$\lambda([\text{X}_2]) = \lambda(0) + k[\text{X}_2], \quad (1)$$

where $\lambda(0)$ is a background relaxation measured in the absence of reagent (X_2). It should be noted that the μSR tech-

nique demands that there be only one muonium atom in the target at a time, leaving the system free of many problems that can plague similar studies of H atom kinetics.^{42,43,51,52} Also see discussions in Refs. 38–40, 46 and 48.

Measurements have been carried out in different target vessels (reactors) designed to operate over the wide temperature range of the experiment. In order to obtain the low temperature data, a triple walled aluminum vessel was employed. The outermost jacket of this vessel was continuously evacuated during the experiments, while the innermost compartment contained the reaction mixture. Air, cooled or warmed to the appropriate temperature by a heat exchanger, was blown through the intermediate jacket. By this technique, temperatures both above and below room temperature could be maintained. However, at temperatures beyond about 400 K, we discovered that both F₂ and Cl₂ reacted with the Al walls of the target vessel, necessitating the use of a target of different design. We initially made use of the same stainless steel (SS) target vessel that is described in Ref. 1, but again discovered that the halogens became chemically reactive at temperatures even as low as 330 K. No amount of "passivation" seemed to help; indeed, we found that stainless steel seems to have an insatiable appetite for F₂ at temperatures ≥ 350 K. This unexpected development mandated a long search for a suitably inert material. In the end, we constructed a cylindrical 16 ℓ nickel-plated copper target vessel for measurements from room temperature to 500 K, which proved to be chemically unreactive to all the halogens (including I₂) up to 550 K. These temperatures were obtained by the use of heating tapes, wrapped on the outside surface of the vessel and thermally insulated. The temperature of the gas mixture was constantly monitored by either chromel–constantan (low temperature range) or iron–constantan (room temperature and above) thermocouples. Temperature gradients over the muons' stopping distribution were measured off-line to be typically 2 °C or better at all temperatures, as duly recorded in Table I below.

In both the Al and the Ni-plated copper vessel, the low energy surface muon beam was admitted through thin (0.005 in) Kapton windows. The window design for the stainless steel vessel was considerably more complicated and is described in Ref. 1.

The reagent gases, obtained from Canadian Liquid Air, had the following purity specifications: F₂, 99.8%; Cl₂, 99.8%; N₂, 99.999%; Ar, 99.999%; and were used without further purification. Liquid Br₂ was obtained from BDH and was subjected to a series of freeze–pump–thaw cycles in order to remove any dissolved O₂, since it is known that this can cause relaxation of the μ SR signal via electron spin exchange.⁶²

In a typical experiment at the higher temperatures, the target vessel was passivated for about 20 min. with about the same (or greater) concentration of X₂ as required in the run to follow. A measured amount of halogen gas was added to the reactor by first filling a smaller vessel of known "standard" volume (SV = 0.104 ℓ) to a desired pressure, as measured by a capacitance manometer, and then flushing this into the previously evacuated target with moderator gas. The same procedure was followed at the low temperatures as

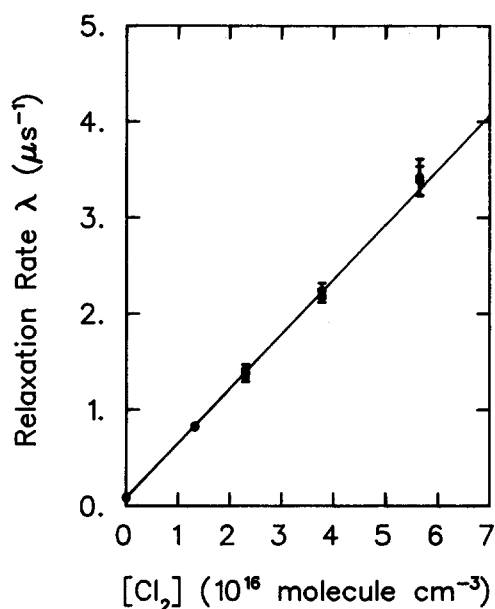


FIG. 1. Relaxation rates (λ_{Mu}) vs Cl₂ concentration for the Mu + Cl₂ reaction at 171 K. The vertical error bars are due to counting statistics. The straight line is a least-squares fit of Eq. (1) to the data, the slope of which yields the thermal bimolecular rate constant of interest $k = (5.64 \pm 0.08) \times 10^{-11} \text{ cm}^3 \text{ molecule}^{-1} \text{ s}^{-1}$ in this case.

well, although the passivation time was generally shorter. A total pressure of 800 Torr (N₂) was used at room temperature and below, whereas the pressure was increased to maintain a density equal to 800 Torr at 298 K in the experiments performed at higher temperatures. While N₂ was used predominantly as a moderator in these experiments, because it gives a large amplitude for Mu precession,^{58,59} for a few runs argon was also used to check for any moderator dependence.⁴⁰ None was found.

In the experiments performed at room temperature and above, the concentration of the X₂ in the gas mixtures was determined by collecting a sample in an evacuated flask, drawing in an excess of potassium iodide solution and titrating the I₂ with thiosulphate, using starch as an indicator.⁶³ This procedure was used as well in a long and tedious series of off-line tests to determine the limits of chemical reactivity of the halogens with metal target vessels, culminating in our choice of the nickel-plated copper vessel described above. In general, the concentrations determined from the titrations agreed well with those calculated from the pressure measurements. No titrations were carried out in the experiments below room temperature.

Measurements of $\lambda(0)$ were made in pure N₂ or Ar at each temperature or during the time taken to change from one temperature to the next. At least three reactant concentrations plus $\lambda(0)$ were used to obtain a plot of λ vs [X₂] at a given temperature, such as is shown in Fig. 1 for Mu + Cl₂ at 171 K. The straight line is a least-squares fit of Eq. (1) to the data, the slope of which yields the thermal bimolecular rate constant of interest.

III. RESULTS

The rate constants for reactions (R1)–(R3) measured at various temperatures are reported in Table I. Each repre-

TABLE I. Experimental rate constants for $\text{Mu} + \text{X}_2$.

	T (K)	k ($10^{-11} \text{ cm}^3 \text{ molecule}^{-1} \text{ s}^{-1}$)	Reaction vessel	
Mu + F ₂ (R1)	450 ± 2	3.77 ± 0.28	Ni	
	380 ± 2	3.03 ± 0.19	Ni	
	298 ± 2	2.66 ± 0.16	Ni	
	297 ± 1	2.61 ± 0.06	A1	
	259 ± 3	2.00 ± 0.04	A1	
	246 ± 1	1.59 ± 0.03	A1	
	228 ± 1	1.58 ± 0.03	A1	
	200 ± 2	1.26 ± 0.02	A1	
	186 ± 1	1.22 ± 0.02	A1	
	165 ± 1.5	1.08 ± 0.02	A1	
	145 ± 1.5	1.01 ± 0.02	A1	
	125.5 ± 1	0.926 ± 0.014	A1	
	125.5 ± 1 ^a	0.901 ± 0.018	A1	
	100.5 ± 1	0.869 ± 0.014	A1	
	Mu + Cl ₂ (R2)	476 ± 2	13.00 ± 0.70	Ni
422 ± 2		13.30 ± 0.80	Ni	
422 ± 2		11.30 ± 0.27	Ni	
406 ± 5		11.30 ± 0.27	SS	
381 ± 2		10.74 ± 0.60	Ni	
380 ± 2		11.63 ± 0.27	Ni	
324 ± 3		9.54 ± 0.22	SS	
298 ± 2		9.67 ± 0.55	Ni	
297 ± 1		8.14 ± 0.19	SS	
297 ± 1		8.75 ± 0.20	A1	
259 ± 3		7.51 ± 0.15	A1	
246 ± 1.5		7.40 ± 0.16	A1	
226 ± 2		6.74 ± 0.12	A1	
200 ± 2		5.91 ± 0.11	A1	
180 ± 1		5.94 ± 0.10	A1	
171 ± 2		5.64 ± 0.08	A1	
165 ± 1.5		5.27 ± 0.09	A1	
158 ± 1.5		5.48 ± 0.09	A1	
Mu + Br ₂ (R3)		447 ± 2	39.90 ± 2.9	Ni
		406 ± 5	53.1 ± 1.3	SS
	380 ± 2	46.5 ± 3.8	Ni	
	324 ± 3	55.8 ± 1.5	SS	
	298 ± 2	55.7 ± 3.1	Ni	
	297 ± 1	57.6 ± 1.6	SS	
	297 ± 1	55.1 ± 1.2	A1	
	259 ± 2	57.3 ± 1.1	A1	
	227 ± 1	58.0 ± 1.2	A1	
	201 ± 1	60.0 ± 0.9	A1	

^a 380 Torr total pressure.

sents a simultaneous fit to Eq. (1) of the relaxation rates from two independent histograms of muon decay events recorded for varying concentrations of the reactant gas. The temperature uncertainties are the measured variations, while the (1σ) uncertainties in the rate constants arise primarily from counting statistics, via uncertainties in the fitted values for relaxation rates from the data histograms. Although these results were obtained in several runs at the TRIUMF cyclotron spanning a period of three years, the level of systematic error is estimated to be at worst 10% by comparing the results for $\text{Mu} + \text{Cl}_2$ at room temperature, obtained in three different target vessels. Similar measurements for both $\text{Mu} + \text{Br}_2$ and $\text{Mu} + \text{F}_2$ are in much better agreement.

The data for $\text{Mu} + \text{X}_2$ in Table I are shown in the form of Arrhenius plots in Fig. 2 (solid points), together with

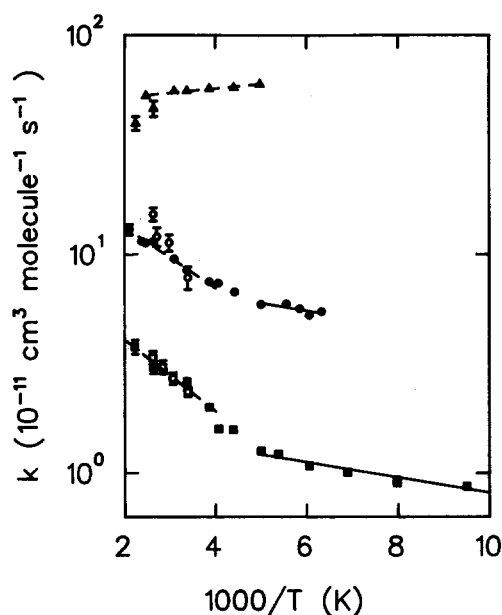


FIG. 2. Arrhenius plots for reactions (R1) (squares), (R2) (circles), and (R3) (triangles). The present data are shown as the solid points, which encompass statistical errors as well. For clarity, data points which overlap at a given temperature (Table I) have been combined. The dashed line segments are Arrhenius fits over 250–500 K for reactions (R1) and (R2) and over 200–400 K for reaction (R3), while the solid lines represent Arrhenius fits over the range 100–200 K for $\text{Mu} + \text{F}_2$ (R1), but over the more restricted range 160–200 K for the $\text{Mu} + \text{Cl}_2$ reaction. The open points for both the $\text{Mu} + \text{F}_2$, Cl_2 reactions are data obtained some years ago in the temperature range ~ 300 – 420 K by Garner and co-workers (Refs. 5, 38, and 39).

least-squares⁶⁴ fits to the usual Arrhenius expression $k = A \exp(-E_a/RT)$, shown as the dashed lines over “high” (250–500 K) and as solid lines over “low” (below 200 K) temperature regions. For F_2 , the low temperatures span a range from 100–200 K, but this range is only from 158–200 K in the case of Cl_2 . The earlier data of Garner and co-workers for $\text{Mu} + \text{Cl}_2$ and $\text{Mu} + \text{F}_2$, obtained in the temperature range 300–420 K,^{5,39,40} are shown as the open points in Fig. 2.

The present data for F_2 agree well with these earlier results. In that study,⁴⁰ an activation energy $E_a = (0.9 \pm 0.2) \text{ kcal mol}^{-1}$ was reported, in good agreement with the present value of $E_a = (0.75 \pm 0.08) \text{ kcal mol}^{-1}$, obtained over the wider range of ~ 250 – 500 K. The present data for reaction (R1) in Fig. 2 were obtained at a room temperature equivalent of 800 Torr (N_2) pressure. Measurements at 380 Torr at 126 K gave no significant change in rate constant (Table I), as expected for a simple abstraction reaction.

The data shown in Fig. 2 for the $\text{Mu} + \text{Cl}_2$ reaction (R2) do not extend to as low temperatures as is the case for F_2 , due to the lower Cl_2 vapor pressure. At higher temperatures, the present data agree with our previously published results,^{5,39} although less satisfactorily than for the F_2 reaction. The earlier Cl_2 data appear to have a greater slope over the temperature range 300–420 K, giving a reported activation energy of $E_a(\text{Mu}) = (1.4 \pm 0.2) \text{ kcal mol}^{-1}$, while the

present data give only half this value $E_a(\text{Mu}) = (0.64 \pm 0.05) \text{ kcal mol}^{-1}$, the same within errors as observed for reaction (R1). However, this discrepancy is predicated largely on the highest temperature (420 K) point of the earlier data, all of which, it is noted, were obtained during the initial stages of operation of the TRIUMF cyclotron and are characterized by much larger uncertainties. Nevertheless, this difference caused us considerable concern since we had discovered during the course of the experiments that the Cl_2 results at temperatures $\geq 350 \text{ K}$ were much less reproducible than the F_2 ones, for reasons that were never clear. We can only attribute inconsistency with the earlier data³⁹ for reaction (R2), particularly that for the 420 K point, to systematic error of unknown origin. Indeed, if this point is discarded, the comparison between the old and new data in Fig. 2 is quite acceptable.

The Arrhenius plot for $\text{Mu} + \text{Br}_2$ extends down to only 200 K, limited even more in this case by the relatively low Br_2 vapor pressure. The Br_2 data in Fig. 2 were reproducible over two data taking periods, with three additional points (Table I) taken in the nickel-plated target vessel in a third period. However, the present room temperature values are about 40% higher than an earlier point (not plotted), taken almost 15 years ago at Berkeley.³⁸ This difference is probably explained by the consistency achieved in the concentrations in the present experiments. Indeed the earlier work used the vapor pressure of bromine above the liquid at a measured temperature to determine the reactant concentration—a method subject to errors both in the accuracy of the temperature measurement and the accuracy of the vapor pressure tables.⁶⁵

IV. THEORETICAL BACKGROUND

In contrast to the $\text{Mu} + \text{H}_2$ reaction,^{1,2,6,7} there are no similarly accurate 3D QM calculations for reaction rates of Mu (or H) with the halogens, although over the years, Connor and co-workers^{11,12,53–57} have done 1D QM and QCT studies of both the activation energies and kinetic isotope effects ($k_{\text{Mu}}/k_{\text{H}}$), particularly comparing reactions (R1) and (R4). Their early 1D calculations^{11,12} were in fact an important motivation for our first experimental studies of these reactions at the TRIUMF cyclotron.^{5,38–40} There have also been 1D–3D distorted-wave Born approximation (DWBA) information theory results⁶⁶ and 1D quantum Franck–Condon calculations⁶⁷ carried out on these reaction systems, but addressing the vibrational populations in the MuX (and HX) products. Like HX,^{29,30,42,68,69} the MuX vibrational distributions could in principle be seen by chemiluminescence experiments; however, there are as yet no such data. It is interesting to note, though, that the calculations provide a dramatic example of the “light atom anomaly,”²⁹ in which the quantum number of the most populated final vibrational state is considerably reduced in the MuX product relative to the HX one.

The most recent calculations of the thermal rate constants for the reaction of both H and Mu atoms with the halogens are the 3D VTST calculations of Steckler, Garrett, and Truhlar.^{13,14} In TST, the kinetic isotope effect (KIE) of interest here may be written^{3,5,17} as

$$\frac{k_{\text{Mu}}}{k_{\text{H}}} = \left(\frac{\kappa_{\text{Mu}}}{\kappa_{\text{H}}} \right) \left[\frac{m_{\text{(H)}}^*}{m_{\text{(Mu)}}^*} \right]^{1/2} \prod_{i=1}^N \frac{\Gamma_{i(\text{Mu})}^\ddagger}{\Gamma_{i(\text{H})}^\ddagger}, \quad (2)$$

where kappa (κ) is a transmission coefficient, m^* denotes the effective mass at the barrier, N is the number of bound vibrational degrees of freedom at the transition state, and Γ_i^\ddagger are essentially the vibrational partition functions at the transition state, which contain the zero point energy differences between Mu and H atom substituted bonds (and hence differences in E_a). Both the position and geometry of the barrier can crucially affect the results of a calculation based on Eq. (2). At a late barrier, the transition state resembles the products and $\Gamma_{\text{(Mu)}}^\ddagger/\Gamma_{\text{(H)}}^\ddagger \rightarrow 0$ and $(m_{\text{(H)}}^*/m_{\text{(Mu)}}^*)^{1/2} \rightarrow 1$. This is qualitatively the situation in our previous study of the highly endothermic $\text{Mu} + \text{H}_2$ reaction.^{1,3} In contrast, since Mu(H) atom reactions with the halogens are highly exothermic, they all have early barriers and as the barrier height falls from F_2 to Br_2 , the barrier becomes earlier.^{13,14,24} Typically, an early barrier gives rise to a slightly perturbed reactant molecule as a transition state, whose vibrations display almost no dependence on isotopic substitution $\Gamma_{\text{(Mu)}}^\ddagger/\Gamma_{\text{(H)}}^\ddagger \rightarrow 1$ and $(m_{\text{(H)}}^*/m_{\text{(Mu)}}^*)^{1/2} \rightarrow 2.9$, simply reflecting the trivial difference in mean collision velocities between Mu and H.

Tunneling can dramatically affect kinetic isotope effects^{8–10,17,70–73} as can recrossing of the dividing surface,^{9,70–74} both effects manifest in the transmission coefficient κ . In VTST, the position of the barrier is varied to minimize the latter effect, which is relatively insignificant on an early barrier surface anyway. The most important aspect of the transmission coefficient for H atom reactions on the halogens is thus quantum tunneling. In general, $\kappa_{\text{Mu}}/\kappa_{\text{H}} \gg 1$ only for a very early barrier since translational energy will be much more effective than vibrational energy in promoting reaction; in this case the reduced mass of the system is essentially just that of the incident atom. Since $m(\text{Mu})/m(\text{H}) = 1/9$, Mu reaction kinetics are much more sensitive to tunneling than are H atom kinetics.

The VTST calculations of Steckler *et al.* are “improved canonical variational theory” (ICVT) calculations⁷⁰ on a variety of LEPS-type surfaces.^{26,28–31,34} Several tunneling paths have been utilized in these calculations to account for the transmission coefficient κ ^{9,13,14,70–73} including the Least Action Ground-state (LAG) path that rather successfully accounted for the $\text{Mu} + \text{H}_2$ data referred to earlier.^{1,2,7,9} In the LAG treatment, the (1D) path that gives the least amount of wave function damping (the most tunneling) is chosen as the optimum tunneling path. Other tunneling paths are approximations to this more exact LAG path; the minimum energy path semiclassical adiabatic ground state (MEPSAG) and the small curvature semiclassical adiabatic ground state (SCSAG) paths, in the notation of Truhlar and co-workers. The MEPSAG is the simplest method and assumes that all tunneling occurs along the MEP (the path of steepest descent). Since this is generally the longest path, it gives the least amount of tunneling (the most damping). The SCSAG method accounts for reaction path curvature, but is expected to be most accurate for reactions where the path curvature is small. These approximations have recently been

discussed in a theoretical study of the H(D) + HBr exchange reaction.⁷³

In the calculations of Steckler and Truhlar,^{13,14} at room temperature the H(Mu) + F₂ reactions show little sensitivity to either the surface Jonathan–Okuda–Timlin (JOT2)²⁸ or Polanyi–Schriber–Sloan (PSS)²⁹ or the kind of tunneling path used, with the LAG and MEPSAG calculations giving essentially identical results and the SCSAG giving only about a 10% increase in calculated rate constants. This insensitivity to the choice of tunneling path was also found to be the case for the Mu(H) + Cl₂ reaction. Since the reaction path curvature is small in the H(Mu) + X₂ reaction systems, it is the SCSAG calculation^{72,73} which is emphasized in Refs. 13 and 14 and which is exclusively referred to in the following.

In contrast to Mu(H) + F₂ though, the results for the Mu(H) + Cl₂ calculations depend considerably on the choice of potential energy surface (PES). In comparing the surfaces of Ding *et al.* (DKPPS),³⁰ Last and Baer (LB),³⁴ and Connor *et al.* (CJMW),²⁶ Steckler *et al.* find that results obtained with the CJMW and DKPPS surfaces are very similar, both giving considerably better agreement with the experimental Mu(H) + Cl₂ data than does the LB surface.

Likely the best experimental indication of quantum tunneling in these reactions can be found in a comparison of the Arrhenius activation energies E_a (Mu) and E_a (H). In accord with the Tolman definition⁷⁵

$$E_a(T) = \frac{d \ln k(T)}{d(1/RT)} = \langle E^* \rangle - \langle E \rangle, \quad (3)$$

where $\langle E^* \rangle$ is the average energy of those molecules which actually lead to reaction, whereas $\langle E \rangle$ is the average energy of all molecules ($3/2 k_B T$ for translations). Classically, $\langle E^* \rangle$ increases with temperature faster than $\langle E \rangle$, leading to a slight increase in E_a with increasing temperature, an effect which is relatively insensitive to changes in isotopic mass (see, e.g., Table III below and Refs. 11, 12, and 53–57). In contrast, in the case of quantum tunneling, $\langle E^* \rangle$ is reduced,

particularly at low temperatures for light mass isotopes (such as Mu), leading to both an isotopic (Tables II, IV, and VI) and temperature-dependent decrease in activation energy. Thus, either classical or quantum effects may be manifest in curvature in the corresponding Arrhenius plot if a wide enough temperature range has been covered.^{10,12,17,53,75}

V. DISCUSSION

The data presented here represent a significant extension not only of the experimental results for the reactions of muonium with the halogens obtained in the mid-70's, but also an important extension of the body of data for thermal reactions of all hydrogen isotopes with the halogens. Before discussing each Mu(H) + X₂ reaction in some detail, it is of interest to first examine both the H and Mu data briefly in order to point out the trends observed. Table II displays the enthalpies for reactions (R1)–(R3); the Mu, H, and D atom rate constants; the kinetic isotope effects KIE(Mu/H) $k_{\text{Mu}}/k_{\text{H}}$ and KIE(H/D) $k_{\text{H}}/k_{\text{D}}$ at room temperature; the experimental ratio of transmission coefficients $\kappa_{\text{Mu}}/\kappa_{\text{H}}$ at room temperature and at about 250 K for Mu and H atom reactions with F₂ and Cl₂ (see Figs. 3 and 4); the Arrhenius activation energies E_a (Mu) for Mu + X₂ determined between about 250 and 500 K and for H + X₂, E_a (H), from the published values^{46–49} over a comparable temperature range; and finally the classical barrier height (V^\ddagger) from Refs. 13 and 14. The trivial KIE of 2.9 for these early barrier reactions [see Eq. (2)] has been factored out in defining $\kappa_{\text{Mu}}/\kappa_{\text{H}}$, which is then a measure of some “dynamical effect” of isotopic substitution on HX₂ kinetics.

The comparisons given in Table II present a considerable challenge to theory for reactions (R1)–(R6). Note first that, although the reaction with F₂ is the most exothermic, it is nevertheless the slowest for both Mu and H, having correspondingly the highest barrier (V^\ddagger) and activation energy (E_a). This anomalous behavior, contravening the Ogg–Polanyi (Mok–Polanyi) relationship,⁷⁶ has recently been explained for H + X₂ in terms of “frontier orbital” theory.⁷⁷

TABLE II. A comparison of data for Mu (H) + X₂.

	F ₂ ^a	Cl ₂ ^b	Br ₂ ^c
ΔH kcal mol ⁻¹	- 88.20	- 37.10	- 34.00
$k_{298}(\text{Mu})$ (10 ⁻¹¹ cm ³ molecule ⁻¹ s ⁻¹) ^d	2.62 ± 0.06	8.50 ± 0.14	56.0 ± 0.9
$k_{298}(\text{H})$ (10 ⁻¹¹ cm ³ molecule ⁻¹ s ⁻¹)	0.16 ± 0.01	2.10 ± 0.10	8.20 ± 3.80
$k_{298}(\text{D})$ (10 ⁻¹¹ cm ³ molecule ⁻¹ s ⁻¹) ^e	...	1.40 ± 0.44	5.6 ± 0.9
KIE ₂₉₈ (Mu/H)	16.4	4.0	6.8
KIE ₂₉₈ (H/D) ^e	...	1.5	1.5
$\kappa_{\text{Mu}}/\kappa_{\text{H}}$ (298 K)	5.7	1.4	2.3
$\kappa_{\text{Mu}}/\kappa_{\text{H}}$ (250 K)	8.0	2.1	...
E_a (Mu) (kcal mol ⁻¹)	0.75 ± 0.08	0.64 ± 0.05	0.095 ± 0.020
E_a (H) (kcal mol ⁻¹)	2.20 ± 0.08	1.20 ± 0.10	...
V^\ddagger (kcal mol ⁻¹) ^e	2.30	1.50	~0

^a H atom data from Homann *et al.* (Ref. 46). See also Fig. 3.

^b H atom data from Bemand and Clyne (Ref. 49) and Wagner *et al.* (Ref. 48). Rate constants and activation energies given as weighted averages. See also Fig. 4.

^c H atom data from Jaffe and Clyne (Ref. 50).

^d k_{298} (Mu) given as weighted average of results in Table I.

^e Barrier heights from Refs. 13 and 14.

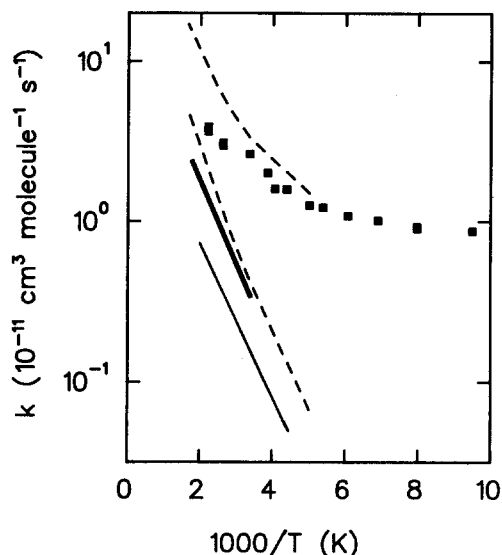


FIG. 3. Arrhenius plot for $\text{Mu} + \text{F}_2$ (squares), together with the VTST calculations of Steckler, Garrett, and Truhlar (Refs. 13 and 14) (top dashed line). Also shown are the H atom data of Albright *et al.* (Ref. 47) (thick solid line) and Homann *et al.* (Ref. 46) (solid line) together with the calculations of Steckler *et al.* for this reaction (lower dashed line).

Secondly, consider the KIEs and corresponding transmission coefficients. Even at room temperature, the ratios $\kappa_{\text{Mu}}/\kappa_{\text{H}} > 1$ for all three comparisons in Table II, although marginally so for Cl_2 , but this dynamical mass effect increases below ~ 250 K, particularly for F_2 . On the other hand, the room temperature KIE $k_{\text{H}}/k_{\text{D}}$ for both reactions (R5) and (R6) is very close to the classical result of 1.4, suggesting no tunneling at all at this temperature. Thirdly, note the difference in activation energies for reactions (R1)/

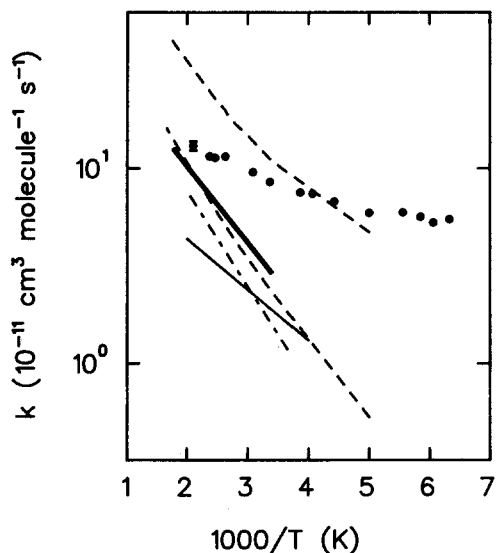


FIG. 4. Arrhenius plot for $\text{Mu} + \text{Cl}_2$ (circles), together with the VTST theory of Steckler, Garrett, and Truhlar (Refs. 13 and 14) for this reaction (top dashed line) and the H atom data from Albright *et al.* (Ref. 47) (double solid line) and Wagner *et al.* (Ref. 48) (solid line). The lower dashed line is from the VTST calculations of Steckler *et al.* for $\text{H} + \text{Cl}_2$. Also shown is the Arrhenius plot from the QCT calculations of Connor *et al.* (Ref. 57) (dotted-dashed line).

(R4) and (R2)/(R5). For $\text{Mu}(\text{H}) + \text{F}_2$, even at the high temperatures, $E_a(\text{Mu})$ is only a third of $E_a(\text{H})$, while it is half of this for $\text{Mu} + \text{Cl}_2$. The Mu activation energies become progressively less at lower temperatures, approaching zero at the lowest temperatures measured (see Fig. 2). In contrast, the H atom activation energies are independent of temperature (see Figs. 3 and 4). These observations demonstrate the important role that quantum tunneling is playing in both the $\text{Mu} + \text{F}_2$ and $\text{Mu} + \text{Cl}_2$ reactions. In marked contrast to the behavior seen for F_2 and Cl_2 , the data for $\text{Mu} + \text{Br}_2$ [reaction (R3)] exhibit the opposite temperature dependence (Fig. 2), indicating a zero potential energy barrier; tunneling must be of little or no consequence here, despite the relatively large room temperature value for $\kappa_{\text{Mu}}/\kappa_{\text{H}}$ in Table II.

The pronounced curvature seen in the Arrhenius plot for the reaction of Mu with F_2 down to 100 K in Fig. 2 (and indicated also for Cl_2 below 160 K), where the rate constant $k_{\text{Mu}}(T)$ appears to be independent of temperature, is likely the most dramatic ever reported for an (H atom) reaction in the gas phase and is strongly indicative of the presence of Wigner threshold tunneling⁷⁸ in these reactions. According to the Wigner threshold law, the excitation function $\sigma(E)$ is proportional to $1/\sqrt{E}$ and thus, like the dependence seen in the Langevin cross section for (long-range) ion-molecule encounters,^{79,80} $k(T)$ becomes temperature independent as $T \rightarrow 0$. The Wigner law should hold if the ratio of the de Broglie wavelength λ to the barrier thickness t is much greater than unity. If λ is expressed in terms of the translational energy, equated to $k_B T$, then T can be obtained⁷⁸ from

$$T \ll h^2 / (2\mu k_B t^2), \quad (4)$$

where μ is the translational reduced mass. Taking t from the PES given in Ref. 13, T need only be smaller than 500 K for $\text{Mu} + \text{F}_2$, a condition easily met by the experiment. It can be remarked that for $\text{H} + \text{F}_2$, the same condition is obtained only at temperatures well below 50 K, far below the range of available data (Fig. 3).

A. Experiment and theory: $\text{Mu}(\text{H}) + \text{F}_2, \text{Cl}_2$

Figures 3 and 4 display Arrhenius plots of the present (Table I) Mu data for reactions (R1) and (R2), respectively (see also Fig. 2), compared with the corresponding H atom data for reactions (R4) and (R5) from the work of both Albright *et al.*⁴⁷ (thick solid lines in both figures) and Homann *et al.* for F_2 ⁴⁶ in Fig. 3, and Wagner *et al.* for Cl_2 ⁴⁸ in Fig. 4 (thin solid lines). As noted earlier, the Albright *et al.* data is judged to be the least reliable,^{44,45} although this statement has been queried in the literature.¹¹⁻¹⁴ The H atom plots in Figs. 3 and 4 were constructed from published Arrhenius parameters over the temperatures indicated.⁴⁶⁻⁴⁸ The dashed lines in both figures are from the recent (SCSAG) ICVT calculations of Steckler *et al.*^{13,14} for both the Mu (upper dashed lines) and $\text{H} + \text{F}_2, \text{Cl}_2$ (lower lines) reactions. The dot-dashed line in Fig. 4 is from the QCT calculations of Connor *et al.* for the $\text{H} + \text{Cl}_2$ reaction.⁵⁷

Both Figs. 3 and 4 reveal several qualitative features important to an understanding of H(Mu) atom reaction dynamics on F_2 and Cl_2 . Their most obvious feature is the pro-

TABLE III. Comparisons of experimental and ICVT/SCSAG rate^a constants for Mu + F₂.

T (K)	$k_{\text{Mu}}(T)$ $10^{-11} \text{ cm}^3 \text{ molecule}^{-1} \text{ s}^{-1}$			KIE (expt.) ^b	KIE (JOT2) ^a
	Expt.	JOT2	PSS		
200	1.26 ± 0.02	1.5	1.5	...	22.6
295	2.62 ± 0.06 ^c	3.3	3.5	16.4	8.1
327	2.72 ^d	4.2	4.4	12.1	6.6
353	2.96 ^d	5.0	5.2	10.2	5.9
383	3.06 ^d	6.1	6.3	8.3	5.2
400	3.36 ^d	6.7	6.9	8.0	4.9
450	3.77 ± 0.28	8.0 ^e	8.2 ^e	6.6	4.0 ^e
600	~4.80 ^f	17	17

^a From Table III, Ref. 14.

^b Assuming H atom data from Homann *et al.* (Ref. 46); from the Arrhenius plot in Fig. 3, this paper.

^c From the 298 K value, Table II.

^d From Arrhenius fit to data in Fig. 2.

^e From Arrhenius fit to JOT2 calculations of Ref. 14.

^f Extrapolated from fit to data in Fig. 2.

nounced curvature in the Mu results, significantly absent in the H atom data (though there seems to be a hint of some curvature in the H + F₂ data of Albright *et al.*^{5,40}). In parallel with the changing slope seen in k_{Mu} , the experimental KIEs (Tables III and V) and hence the ratio of transmission coefficients $\kappa_{\text{Mu}}/\kappa_{\text{H}}$ are $\gg 1$ at the lowest temperatures (Table II). In both F₂ and Cl₂, the ICVT calculations of Steckler *et al.*^{13,14} fail to account for the trend in the Mu data at the higher temperatures, although (perhaps fortuitously) good agreement is obtained at selected temperatures near 250 K. These calculations also overestimate the H atom data of Homann *et al.* (Fig. 3) and Wagner *et al.* (Fig. 4), but curiously the ICVT calculations agree rather well with the data of Albright *et al.* for both F₂ and Cl₂, over the whole temperature range (Figs. 3 and 4).

Table III compares the experimental rate constants $k_{\text{Mu}}(T)$ for Mu + F₂ with the ICVT/SCSAG calculated values of Steckler *et al.* on the JOT2²⁸ and PSS²⁹ potential surfaces. It is clear there is little sensitivity to the choice of PES for this reaction, so the JOT2 results alone are plotted in

Fig. 3 for both reactions (R1) and (R4). As can be seen in this figure, there is a clear divergence at the higher temperatures, with the calculated rates becoming progressively too large. If anything, the calculations for k_{H} are in even worse agreement with experiment, assuming the H atom data of Homann *et al.*,⁴⁶ and, correspondingly, the calculated KIEs in Table III tend to fall below the experimental results by about a factor of 2 over the whole temperature range.

The earlier 1D QM calculations of Connor *et al.*^{5,11,12,40} are "exact" in a collinear world and are compared with the experimental KIEs and E_a 's in Table IV. These calculations have also employed the JOT2 PES²⁸ for reactions (R1) and (R4) and reproduce the same trend in $k_{\text{Mu}}/k_{\text{H}}$ that is seen in the data as the 3D VTST calculations of Steckler *et al.* (Table III), which may be taken as some confirmation of the dominance of collinear reaction dynamics in Mu(H) + F₂. In both cases, however, the calculated ratio is too low; the theoretical rate constants appear to underpredict the amount of tunneling seen in the Mu data. This can also be seen from a comparison of the 1D activation energies in Ta-

TABLE IV. Collinear rate constants and activation energies for Mu(H) + F₂.

T (K)	$k_{\text{Mu}}/k_{\text{H}}$		$E_a(\text{Mu})$		$E_a(\text{H})$	
	Theory ^a	Expt. ^b	Theory ^a	Expt. ^c	Theory ^a	Expt. ^c
200	16.40	0.16 ± 0.08
300	5.90	16.4	1.11	0.75 ± 0.08	2.06	2.20 ± 0.08
550	3.30	4.9 ^d	1.89	...	2.49	...
900	2.80	...	2.54	...	2.89	...

^a From the 1D QM calculations of Connor and co-workers (Refs. 11, 12, and 53).

^b H atom data taken from the work of Homann *et al.* (Ref. 46). The corresponding ratios from the data of Albright *et al.* (Ref. 47) would be about a factor of 2 smaller over the whole temperature range. See comparative plots in Fig. 3. Muonium data from this work.

^c H atom activation energy from Ref. 46. However, this agrees well with that of Albright *et al.* (Ref. 47). See Fig. 3. Muonium data from this work. Both in units of kcal mol⁻¹. The $E_a(\text{H})$ is independent of temperature. The $E_a(\text{Mu})$ have been calculated from Arrhenius fits over a range of temperature spanning the tabulated mid points, as defined in Ref. 12.

^d From extrapolation of Arrhenius fits in Figs. 2 and 3.

TABLE V. Comparison of experimental and ICVT/SCSAG rate constants for Mu + Cl₂.

T (K)	$k_{\text{Mu}}(T)$ $10^{-11} \text{ cm}^3 \text{ molecule}^{-1} \text{ s}^{-1}$			KIE (expt.) ^b	KIE (DKPPS) ^a
	Expt.	DKPPS ^a	CJMW ^a		
200	5.91 ± 0.11	4.7	4.6	...	8.4
295	8.50 ± 0.14 ^c	11	11	4.0	4.7
336	9.75 ^d	15	15	4.0	4.2
370	10.50 ^d	18	18	3.7	3.8
381	11.48 ± 0.25 ^e	20	21	3.8	3.8
400	11.20 ^d	22	21	3.5	3.7
600	15 ^f	49	47

^a From Table IV, Ref. 14.

^b Using H atom data of Wagner *et al.* (Ref. 48); from Arrhenius plot in Fig. 4, this paper.

^c From 298 K value, Table II.

^d From Arrhenius fit to data in Fig. 2.

^e Weighted average of results from Table I.

^f Extrapolated from fit to data in Fig. 2.

ble IV: the calculated value for E_a (Mu) at 300 K is significantly higher than the experimental number. On the other hand, these calculations do reproduce the trend seen in the differences in activation energies for Mu + F₂ and H + F₂. It can also be noted that the 1D calculated value for E_a (Mu) approaches that for E_a (H) at 900 K, as expected classically [Eq. (3)], and seen also in QCT calculations comparing reactions (R1) and (R4).^{53–55}

The ICVT calculations for Mu + Cl₂ on the DKPPS³⁰ (plotted) and CJMW²⁶ surfaces, compared in Table V, agree well with each other and with the data at temperatures of approximately 250 K (Fig. 4), but overestimate the data at the higher temperatures, in this case by about a factor of 3. Similarly, as shown in Fig. 4, the ICVT calculations for k_{H} are also higher than the recommended experimental results of Wagner *et al.*⁴⁸ and Bemand and Clyne⁴⁹ (but, curiously again, agree very well with the data of Albright *et al.*⁴⁷). In contrast to the F₂ case, though, the calculated KIEs for Cl₂ in Table V are in good agreement with the data. The QCT calculations for H + Cl₂ by Connor *et al.*⁵⁷ on the CJMW surface (dot-dashed line in Fig. 4) give essentially the same slope as the ICVT ones of Steckler *et al.*, but actually agree better with the magnitude of the experimental rate constants of Wagner *et al.*⁴⁸ near room temperature. Although there is clear disagreement between the ICVT theory and the experimental values of k_{Mu} and k_{H} for both F₂ and Cl₂ at most temperatures, the relative trend to higher rate constants for Mu(H) + Cl₂ compared to F₂ is well reproduced by these calculations, reflecting the fact that the potential barrier is higher for HF₂ than for HCl₂ (Table II). A higher barrier for F₂ is also predicted by *ab initio* calculations, which tend, however, to give barrier heights that are much too high.^{13,14,23,24}

Table VI shows the H and Mu higher temperature 250–500 K and low temperature (< 200 K) activation energies for both F₂ and Cl₂ with the high temperature ICVT calculated values. For H + F₂, theory and experiment are in good agreement; but not so for Mu + F₂, where the theoretical value for E_a (Mu) is a factor of 2 too high. The 1D QM

calculations reported in Table IV are in better agreement with experiment here, suggesting a problem with the tunneling path in the ICVT calculations. On the other hand, both the 1D QM and ICVT calculations do show considerably enhanced tunneling for Mu compared to H, giving lower Mu activation energies. This situation for Mu + F₂ is paralleled by Mu + Cl₂. It can be pointed out though, like the experimental results, the ICVT calculated values of E_a (Mu) are the same for both F₂ and Cl₂.

Despite the level of agreement, or lack thereof, between experiment and the ICVT calculations of Steckler *et al.*,^{13,14} or the 1D QM ones of Connor *et al.*, the real test of these calculations will lie in their ability to account for the muonium data below 200 K. The experimental Arrhenius plots (Fig. 2) deviate strongly from Arrhenius behavior; the high temperature activation energies are reduced by factors of 4 (Cl₂) to 5 (F₂) below 200 K. Unfortunately, theory has not (yet) been extended to these lower temperatures. The present ICVT calculations, particularly for Mu + F₂ (Fig. 3), do exhibit some curvature at the lower temperatures, but indications are from the trend in the theory (e.g., if the barrier height were increased slightly) that the calculations would severely underpredict the amount of tunneling seen in

TABLE VI. Comparison of experimental and theoretical activation energies E_a (Mu) and E_a (H) for Mu(H) + F₂, Cl₂.

T	F ₂		Cl ₂	
	H	Mu	H	Mu
300–500 K				
E_a (exp) ^a	2.2 ± 0.2	0.75 ± 0.08	1.2 ± 0.1	0.64 ± 0.05
E_a (ICVT) ^b	2.6	1.5	2.1	1.5
< 200 K				
E_a (exp) ^c		0.16 ± 0.08		0.16 ± 0.04

^a See Table II, this paper.

^b From calculations of Steckler *et al.* (Refs. 13 and 14).

^c H atom data does not extend below 200 K. Mu activation energies obtained from midpoint fits to temperature ranges indicated in Fig. 2.

the data if extended below 200 K—underpredicting the rate constants and overpredicting the activation energy.

We conclude that either the tunneling path or the topography, hence the vibrational frequencies, of the PES near the barrier are incorrect for both the $\text{Mu} + \text{F}_2$ (JOT2 or PSS surface) and $\text{Mu} + \text{Cl}_2$ (DKPPS or CJMW surface) ICVT calculated results. Although the LAG principle of choosing tunneling paths, as well as the SCSAG approximation to it,⁷³ was quite successful for the $\text{Mu} + \text{H}_2$ reaction,^{1,6–9} tunneling paths in TST are much more stringently tested by the present study on early barrier HX_2 surfaces. The suggestion that the surfaces themselves may be at fault, despite their early success in explaining chemiluminescent data for the corresponding H atom reactions,^{29,30,68} receives some support from the fact that the (exact) 1D QM calculations of Connor *et al.* for $\text{Mu} + \text{F}_2$ in Table IV also failed to account for the isotope effect. A thinner and somewhat higher barrier for reactions (R1) and (R2) would have the effect of reducing k_{Mu} at higher temperatures, where tunneling is relatively unimportant, possibly enhancing it at lower temperatures, and also lowering the value for k_{H} for reactions (R4) and (R5); improving the agreement with experiment in each case. The ICVT calculations^{13,14} must clearly be extended to temperatures well below 200 K in order to critically examine these statements.

The ratio of the Mu and H experimental activation energies for F_2 at high temperatures is $E_a(\text{H})/E_a(\text{Mu}) \approx 3$, compared with ≈ 2 for Cl_2 at the same temperatures (Tables II and VI), suggesting that quantum tunneling is more pronounced in $\text{Mu} + \text{F}_2$ than in $\text{Mu} + \text{Cl}_2$. This is not a surprising result since the classical barrier for F_2 is higher (Table II), revealed by the difference in experimental H atom activation energies for reactions (R4) and (R5), and seen also in abstraction reactions by OH from the halogens.⁸¹ The expectation that there should be relatively more tunneling in $\text{Mu} + \text{F}_2$ than in $\text{Mu} + \text{Cl}_2$ is reflected also in the trends seen in the ICVT calculations of Steckler *et al.*^{13,14} in Table VII, where the experimental and theoretical ratios of transmission coefficients at room temperature are compared. The theoretical κ 's come from a comparison of the ICVT calculations with (SCSAG path) and without tunneling from Table I in Ref. 13. From the calculated ratio $\kappa_{\text{Mu}}/\kappa_{\text{H}}$ in Table VII, there is a factor of 2 more tunneling expected for F_2 than Cl_2 , which is certainly in the right direction, but in poor agreement with the experimental difference of almost a factor of five: $\kappa_{\text{Mu}}/\kappa_{\text{H}} = 5.7$ for F_2 , but only 1.4 for Cl_2 . One might expect though, in view of their considerable difference in

barrier heights, to see $E_a(\text{Mu})$ significantly greater for F_2 than Cl_2 , as in the corresponding H atom experiments. Differences in tunneling must account for the similarity in $E_a(\text{Mu})$ for Cl_2 and for F_2 , which are the same within errors over the whole temperature range studied (Table VI), a result that is accounted for by the ICVT calculations.

B. Experiment and theory: $\text{Mu}(\text{H}) + \text{Br}_2$

In striking contrast to both the $\text{Mu} + \text{F}_2$ and $\text{Mu} + \text{Cl}_2$ reactions, the reaction rate of Mu with Br_2 (R3) decreases with increasing temperature (Fig. 2), giving the apparent negative activation energy quoted earlier [$E_a(\text{Mu}) = (-0.095 \pm 0.020)$ kcal mol⁻¹]. Although this is a small number, it is significant. The data for reaction (R3) have been fit in the range 200–400 K because the highest temperature point at 447 K is well below the line, indicating a more negative slope. Correcting for the $T^{1/2}$ dependence of the collision frequency gives $E_a(\text{Mu}) = (-0.36 \pm 0.02)$ kcal mol⁻¹, emphasizing even more the negative temperature dependence seen in the $\text{Mu} + \text{Br}_2$ reaction.

It is important to note that early atomic beam studies⁸² of reaction (R6) also found this same trend: a decrease in reactive cross section with increasing energy in the range 0.8–8 kcal mol⁻¹. These results and the present Mu data indicate a PES dominated by a long-range attractive potential, as typified, e.g., by radical–radical⁸⁰ or ion–molecule reactions,^{79,80} where cross sections are known to decrease with increasing translational energy. However, this would lead one to expect very large cross sections, $\sim 100 \text{ \AA}^2$ at thermal energies, leading to an expected collision controlled rate constant for $\text{Mu}(\text{H}) + \text{Br}_2$ of order $6 \times 10^{-9} \text{ cm}^3 \text{ s}^{-1}$ at 295 K, an order of magnitude greater than the observed value for Mu. The observed muonium rate constant is seven times higher than the only direct measurement of the $\text{H} + \text{Br}_2$ rate at 295 K⁵⁰ indicative of some dynamical mass effect enhancing the Mu reaction rate by about a factor of 2. This is an even greater enhancement than that seen for Cl_2 , although the large error in the value of k_{H} for reaction (R6) must be kept in mind. The origin of the enhancement for k_{Mu} in $\text{Mu} + \text{Br}_2$ is not at all clear; quantum tunneling should be negligible in this reaction and the corresponding ratio $k_{\text{H}}/k_{\text{D}}$ from the data of Jaffee and Clyne⁵⁰ is just the classically expected result 1.5.

Garrett *et al.*¹⁴ have recently calculated the ICVT $\text{Mu} + \text{Br}_2$ and $\text{H} + \text{Br}_2$ reaction rates at 295 K, using the 19M PES of Blais and Truhlar.³¹ Their values are compared

TABLE VII. Room temperature transmission coefficients (κ) for $\text{Mu}(\text{H}) + \text{F}_2, \text{Cl}_2$.

Quantity	$\text{Mu}(\text{H}) + \text{F}_2$	$\text{Mu}(\text{H}) + \text{Cl}_2$
$\kappa_{\text{Mu}}/\kappa_{\text{H}}$ (exp.) ^a	5.7	1.4
κ_{Mu} (SGT) ^b	5.3	2.1
κ_{H} (SGT) ^b	1.4	1.1
$\kappa_{\text{Mu}}/\kappa_{\text{H}}$ (SGT) ^b	3.8	1.9

^a From Table II, this paper, room temperature values.

^b From calculations of Steckler, Garrett, and Truhlar (SGT), Table I, Refs. 13 and 14.

TABLE VIII. Comparison of experimental and ICVT/SCSAG rate constant for $\text{Mu}(\text{H}) + \text{Br}_2$ at room temperature.

k ($10^{-10} \text{ cm}^3 \text{ molecule}^{-1} \text{ s}^{-1}$)		
	Mu	H
Expt. ^a	5.6 ± 0.1	0.82 ± 0.38
Calc. ^b	17	6

^a Table II, this paper.

^b Table VI, Ref. 14.

with the experimental data in Table VIII. In contrast to both HF_2 and HCl_2 , this surface is noncollinear, with a favored angle of approach by $\text{H}(\text{Mu})$ of about 20° and with no barrier in this direction (the corresponding collinear surface has a barrier of ~ 2.5 kcal/mol, agreeing with *ab initio* calculations.^{24,31,83} The lack of a barrier suggests little or no temperature (energy) dependence in the reaction rate, as observed in the Mu data (Fig. 2). By adjusting the shape of the attractive part of the potential, effectively making it longer range, Blais and Truhlar,³¹ in their QCT calculations, were successfully able to account for both the energy dependence in the H atom beam data of Hepburn *et al.*⁸² and the isotopic ratio $k_{\text{H}}/k_{\text{D}}$ measured by Jaffe and Clyne.⁵⁰ However, the magnitude of the 295 K calculated rate constants were high by about a factor of 3 in both cases. Interestingly, the agreement between experiment and the later ICVT calculations¹⁴ for k_{H} is considerably worse than in the (presumably less accurate) QCT calculation; [$k_{\text{H}}(\text{ICVT}) = 6 \times 10^{-10}$] about a factor of 10 too high. This indicates a problem with the bend potential in HBr_2 ; or with the location of the barrier. Similarly, $k_{\text{Mu}}(\text{ICVT}) = 17 \times 10^{-10}$ is too high, but only by a factor of 3 in this case (see Table VIII). Unfortunately, there have (as yet) been no theoretical calculations of the temperature dependence of the $\text{Mu} + \text{Br}_2$ reaction rate. In the QCT calculations of Blais and Truhlar, there is a small positive activation energy [$E_a(\text{H}) \approx 0.2$ kcal mol⁻¹], in which $E_a(\text{D}) > E_a(\text{H})$ is also predicted, but there is no reliable experimental data to compare with. An assessment of older data in the literature³¹ suggests that $E_a(\text{H})$ should indeed be positive, in marked contrast to the present $\text{Mu} + \text{Br}_2$ results (Fig. 4).

The discrepancy between theory and experiment in both the H and Mu kinetic data suggests that either there is a pronounced "steric effect," or that a long-lived MuBr_2 complex is formed. In the first instance, since the lighter Mu atom has a shorter interaction time than H, it may be more sensitive to specific orientations of a quickly rotating Br_2 molecule. In the latter case, if a complex is indeed formed, it is interesting to speculate that the present results may represent the first experimental evidence of the formation of a Br-Mu-Br bond, which could have several vibrationally bound states.⁸⁴ If so, it may live long enough to give rise to the observed negative temperature dependence seen in the data. Here the mechanism for spin relaxation may be more complex, involving intramolecular couplings in the muonated radical formed.⁸⁵ The formation of such a long-lived complex would also indicate a different HBr_2 bend potential than found in the (19M) PES of Blais and Truhlar, possibly explaining the aforementioned inconsistency between k_{H} in the QCT³¹ and ICVT¹⁴ calculations. Another explanation for the observation of reduced rate constants with increasing temperature might be reflection off the repulsive wall, particularly on a zero barrier surface, thereby reducing the reactive cross section at higher energies. This has been found in QCT calculations for $\text{Mu} + \text{F}_2$ at higher translational energies.⁵⁵ On the other hand, one would presumably expect this effect to give rise to Mu cross sections even smaller than those for H atom scattering, contrary to observations from the corresponding rate constants.

VI. CONCLUSIONS

There are two principal observations to be drawn from this work. Although exhibiting positive activation energies, the Arrhenius plots for both the $\text{Mu} + \text{Cl}_2$ and $\text{Mu} + \text{F}_2$ reactions demonstrate that they are dominated by quantum tunneling at low temperatures, an effect not seen in either of the corresponding H atom reactions (Figs. 2–4). In contrast, the thermal rate constants for the $\text{Mu} + \text{Br}_2$ reaction increase slightly with decreasing temperature, giving rise to an apparent negative activation energy [$E_a = (-0.09 \pm 0.02)$ kcal mol⁻¹].

In comparing the KIEs for $\text{Mu}(\text{H}) + \text{X}_2$ reaction kinetics, the ratios of transmission coefficients $\kappa_{\text{Mu}}/\kappa_{\text{H}}$, which reflect "dynamical" mass effects, are invariably greater than 1, even at room temperature. In the case of F_2 and Cl_2 , $\kappa_{\text{Mu}}/\kappa_{\text{H}}$ increases dramatically with decreasing temperature, particularly for F_2 , reflecting the pronounced quantum tunneling seen only in the Mu reaction. Concomitantly, the activation energies for $\text{Mu} + \text{F}_2(\text{Cl}_2)$ are considerably smaller than those for the corresponding H atom reactions at all temperatures, with $E_a(\text{Mu})$ approaching zero for $\text{Mu} + \text{F}_2$ at temperatures ~ 100 K, indicating the prevalence of Wigner threshold tunneling.⁷⁸

Neither the early 1D QM calculations of Connor and co-workers (Table IV) nor the more recent 3D variational TST (ICVT) calculations of Steckler *et al.* (Tables III and V), in which a small curvature approximation to the tunneling path (SCSAG) is utilized,^{13,14,73} are able to account for either the Mu or H atom data on F_2 or Cl_2 over the range of temperatures studied. Unfortunately, the ICVT calculations have not (yet) been extended below 200 K, where Mu exhibits pronounced quantum tunneling. Extrapolations of present theoretical rate constants fall considerably below the experimental values (Figs. 3 and 4), indicating that either the topography of the HF_2 and HCl_2 PES are incorrect, particularly in the region of the barrier, or the (SCSAG) tunneling path in the TST calculations is inaccurate for these reactions, or both. It would also be of interest to extend the earlier 1D QM calculations of Connor and co-workers^{11,12,53} for $\text{Mu}(\text{H}) + \text{F}_2$ down to these lower temperatures in order to further assess the dominant role being played by quantum tunneling.

In the case of the $\text{Mu}(\text{H}) + \text{Br}_2$ reaction, even at room temperature the ratio of transmission coefficients ($\kappa_{\text{Mu}}/\kappa_{\text{H}}$) indicates a dynamical mass effect favoring Mu reactivity by more than a factor of 2. The origin of this enhancement is not at all clear. Unlike the situation in F_2 or Cl_2 , the negative activation energy for $\text{Mu} + \text{Br}_2$ indicates a zero potential barrier, consistent with early atomic beam data,⁸² and with the PES used to calculate both the H and $\text{Mu} + \text{Br}_2$ rate constants.¹⁴ As such, quantum tunneling should be negligible. It may be that Mu is more sensitive to specific orientations of the noncollinear $\text{H}(\text{Mu})\text{Br}_2$ surface, resulting in a favorable steric effect for Mu reactivity, but one which nevertheless reduces the rate constant considerably from the expected collision controlled limit. Alternatively, a relatively long-lived MuBr_2 complex may form, perhaps sustaining some vibrationally bound states.⁸⁴

In the near future, the $\text{Mu} + \text{I}_2$ reaction will be studied,

in the temperature range above room temperature. Present results with Br_2 suggest that this reaction should also exhibit a negative activation energy, although in this case there are $\text{H} + \text{I}_2$ data available over a reasonably wide temperature range⁸⁶ to compare with. It is noted that these data exhibit an essentially zero activation energy, with a rate constant that is, curiously, about 10 times faster than the $\text{H} + \text{Br}_2$ rate.⁵⁰ In the cases of both $\text{Mu} + \text{Br}_2$ and I_2 , it will be important to check for any pressure dependence to the observed rate constants, particularly at the highest temperatures.

ACKNOWLEDGMENTS

We would like to acknowledge the contributions made by Keith Hoyle and John Worden in support of these experiments, as well as assistance received from Jim Chesko and Ian Gilchrist. We would also like to thank George Schatz for pointing out that the $\text{Mu} + \text{F}_2$ data at the lowest temperatures may indicate the existence of Wigner threshold tunneling. The financial support of NSERC (Canada) is gratefully acknowledged. Acknowledgment is also made, with thanks, to the Donors of the Petroleum Research Fund, administered by the American Chemical Society, for their partial support of this research. One of the authors DGF would also like to express thanks to the Canada Council for their awarding of a Killam Research Fellowship.

- ¹I. D. Reid, D. M. Garner, Y. T. Lee, M. Senba, D. J. Arseneau, and D. G. Fleming, *J. Chem. Phys.* **86**, 5578 (1987).
- ²J. J. Valentini and D. L. Phillips, in *Advances in Gas Phase Photochemistry and Kinetics*, edited by M. N. R. Ashfold and J. E. Baggott (Royal Society of Chemistry, London, 1989), Vol. 2.
- ³D. M. Garner, D. G. Fleming, and R. J. Mikula, *Chem. Phys. Lett.* **121**, 80 (1985).
- ⁴E. Roduner, *Prog. React. Kin.* **14**, 1 (1986).
- ⁵D. M. Garner, Ph.D. thesis, University of British Columbia, 1979.
- ⁶G. C. Schatz, in *Theory of Chemical Reaction Dynamics*, edited by D. C. Clary, (Reidel, Dordrecht, 1986), p. 1.
- ⁷G. C. Schatz, *J. Chem. Phys.* **83**, 3441 (1985).
- ⁸D. K. Bondi, D. C. Clary, J. N. L. Connor, B. C. Garrett, and D. G. Truhlar, *J. Chem. Phys.* **76**, 4986 (1982).
- ⁹B. C. Garrett and D. G. Truhlar, *J. Chem. Phys.* **81**, 309 (1984).
- ¹⁰W. Jakubetz, *J. Am. Chem. Soc.* **101**, 298 (1979); *Hyperfine Interact.* **6**, 387 (1979).
- ¹¹J. N. L. Connor, W. Jakubetz, and J. Manz, *Chem. Phys. Lett.* **45**, 265 (1977).
- ¹²J. N. L. Connor, W. Jakubetz, and J. Manz, *Chem. Phys.* **28**, 219 (1978).
- ¹³R. Steckler, D. G. Truhlar, and B. C. Garrett, *Int. J. Quantum Chem. Symp.* **20**, 495 (1986).
- ¹⁴B. C. Garrett, R. Steckler, and D. G. Truhlar, *Hyperfine Interact.* **32**, 779 (1986).
- ¹⁵B. Brocklehurst and B. D. Cook, *Chem. Phys. Lett.* **142**, 329 (1987).
- ¹⁶T. Oi, A. Popowicz, and T. Ishida, *J. Phys. Chem.* **90**, 3080 (1986).
- ¹⁷H. S. Johnston, *Gas Phase Reaction Theory* (Ronald, New York, 1966).
- ¹⁸M. R. A. Blomberg and B. Liu, *J. Chem. Phys.* **82**, 1050 (1985).
- ¹⁹D. G. Truhlar and C. J. Horowitz, *J. Chem. Phys.* **68**, 2446 (1978).
- ²⁰M. C. Lin, M. E. Umstead, and D. Djeu, *Annu. Rev. Phys. Chem.* **34**, 557 (1983).
- ²¹J. C. Polanyi, J. J. Sloan, and J. Wanner, *Chem. Phys.* **13**, 1 (1976).
- ²²P. J. Kuntz, in *Modern Theoretical Chemistry*, edited by W. H. Miller (Plenum, New York, 1970), Part B, Vol. 2, p. 53.
- ²³H. F. Schaefer, in *Atom Molecule Collision Theory: Guide for the Experimentalist*, edited by R. B. Bernstein (Plenum, New York, 1979), Chap. 2.
- ²⁴R. A. Eades, T. H. Dunning, Jr., and D. A. Dixon, *J. Chem. Phys.* **75**, 2008 (1981); R. A. Eades, Ph.D. thesis, University of Minnesota, 1983.
- ²⁵J. N. L. Connor, *Comput. Phys. Commun.* **17**, 117 (1979).
- ²⁶J. N. L. Connor, W. Jakubetz, J. Manz, and J. C. Whitehead, *J. Chem. Phys.* **72**, 6209 (1980).
- ²⁷B. M. D. Jansen op de Haar, G. G. Balin-Kurti, and R. E. Wyatt, *J. Phys. Chem.* **89**, 4007 (1985).
- ²⁸N. Jonathan, S. Okuda, and D. Timlin, *Mol. Phys.* **24**, 1143 (1972).
- ²⁹J. C. Polanyi, J. L. Schriber, and J. J. Sloan, *Chem. Phys.* **9**, 403 (1975).
- ³⁰A. M. G. Ding, L. J. Kirsch, D. S. Perry, J. C. Polanyi, and J. L. Schreiber, *J. Chem. Soc. Faraday Discuss.* **55**, 252 (1973).
- ³¹N. C. Blais and D. G. Truhlar, *J. Chem. Phys.* **83**, 5546 (1985).
- ³²W. Jakubetz, *Chem. Phys.* **35**, 129 (1978).
- ³³R. L. Wilkins, *J. Chem. Phys.* **63**, 2963 (1975).
- ³⁴I. Last, *Chem. Phys.* **69**, 193 (1982); I. Last and M. Baer, *Int. J. Quantum Chem.* **29**, 1067 (1986).
- ³⁵J. J. Duggan and R. Grice, *J. Chem. Soc. Faraday Trans.* **2** **80**, 729 (1984).
- ³⁶N. C. Firth and R. Grice, *J. Chem. Soc. Faraday Trans.* **2** **83**, 1011 (1987).
- ³⁷I. Last and M. Baer, *J. Chem. Phys.* **80**, 3246 (1984).
- ³⁸D. G. Fleming, J. H. Brewer, D. M. Garner, A. E. Pifer, T. Bowen, D. A. Delise, and K. M. Crowe, *J. Chem. Phys.* **64**, 1281 (1976).
- ³⁹D. G. Fleming, D. M. Garner, J. H. Brewer, J. B. Warren, G. M. Marshall, A. E. Pifer, and T. Bowen, *Chem. Phys. Lett.* **48**, 393 (1977).
- ⁴⁰D. M. Garner, D. G. Fleming, and J. H. Brewer, *Chem. Phys. Lett.* **55**, 163 (1978).
- ⁴¹D. G. Fleming, D. M. Garner, L. C. Vaz, D. C. Walker, J. H. Brewer, and K. M. Crowe, *ACS Adv. Chem. Ser.* **175**, 279 (1979).
- ⁴²R. J. Malins and D. W. Setser, *J. Chem. Phys.* **73**, 5666 (1980).
- ⁴³J. P. Sung, R. J. Malins, and D. W. Setser, *J. Phys. Chem.* **83**, 1007 (1979).
- ⁴⁴N. Cohen and K. R. Westberg, *J. Phys. Chem. Ref. Data* **12**, 532 (1983).
- ⁴⁵R. T. Watson, *J. Chem. Phys. Ref. Data* **6**, 871 (1977).
- ⁴⁶R. H. Homann, H. Schweinfurth, and J. Warnatz, *Ber. Bunsenges. Phys. Chem.* **81**, 724 (1977).
- ⁴⁷R. G. Albright, A. F. Dodonov, G. K. Lavrovskaya, I. I. Morosov, and V. L. Tal'rose, *J. Chem. Phys.* **50**, 3632 (1969).
- ⁴⁸H. Gg. Wagner, U. Welzbocher, and R. Zellner, *Ber. Bunsenges. Phys. Chem.* **80**, 902 (1976).
- ⁴⁹P. B. Bemand and M. A. A. Clyne, *J. Chem. Soc. Faraday Trans.* **2** **73**, 394 (1977).
- ⁵⁰S. Jaffe and M. A. A. Clyne, *J. Chem. Soc. Faraday Trans.* **2** **77**, 531 (1981).
- ⁵¹P. F. Ambidge, J. N. Bradley, and D. A. Whytoch, *J. Chem. Soc. Faraday Trans.* **1** **72**, 1157 (1976).
- ⁵²J. V. Michael and J. H. Lee, *Chem. Phys. Lett.* **51**, 303 (1977).
- ⁵³J. N. L. Connor, W. Jakubetz, and A. Lagana, *J. Phys. Chem.* **83**, 73 (1979).
- ⁵⁴J. N. L. Connor, C. J. Edge, and A. Lagana, *Mol. Phys.* **46**, 1231 (1982).
- ⁵⁵J. N. L. Connor, A. Lagana, A. F. Turfa, and J. C. Whitehead, *J. Chem. Phys.* **75**, 3301 (1981); J. N. L. Connor (private communications).
- ⁵⁶J. N. L. Connor and A. Lagana, *Mol. Phys.* **38**, 657 (1979).
- ⁵⁷J. N. L. Connor, W. Jakubetz, A. Lagana, J. Manz, and J. C. Whitehead, *Chem. Phys.* **65**, 29 (1982).
- ⁵⁸D. G. Fleming, D. M. Garner, and R. J. Mikula, *Phys. Rev. A* **26**, 2527 (1982).
- ⁵⁹D. J. Arseneau, D. M. Garner, M. Senba, and D. G. Fleming, *J. Phys. Chem.* **88**, 3688 (1984); D. J. Arseneau, M.Sc. thesis, University of British Columbia, 1984.
- ⁶⁰D. C. Walker, *Muon and Muonium Chemistry* (Cambridge University, Cambridge, 1983).
- ⁶¹R. Duchovic, A. F. Wagner, R. E. Turner, D. M. Garner, and D. G. Fleming, *J. Chem. Phys.* (submitted).
- ⁶²M. Senba, D. G. Fleming, D. J. Arseneau, D. M. Garner, and I. D. Reid, *Phys. Rev. A* **39**, 3871 (1989).
- ⁶³V. Casella, T. Ido, A. P. Wolf, J. S. Fowler, R. R. MacGregor, and T. J. Ruth, *J. Nucl. Medicine* **21**, 750 (1980); G. T. Bida, R. L. Ehrenkauffer, A. P. Wolf, J. S. Fowler, R. R. MacGregor, and T. J. Ruth, *ibid.* **21**, 758 (1980).
- ⁶⁴F. James and M. Roos, MINUIT, CERN Computer 7600 Interim Programme Library, Geneva (1971).
- ⁶⁵A. N. Nesmeinov, in *Vapor Pressure of the Chemical Elements*, edited by R. Gary (Elsevier, New York, 1963).
- ⁶⁶D. C. Clary and J. N. L. Connor, *J. Chem. Phys.* **75**, 3329 (1980).
- ⁶⁷A. Lagana, *J. Chem. Phys.* **86**, 5523 (1987).

- ⁶⁸J. C. Polanyi and J. J. Sloan, *J. Chem. Phys.* **57**, 4988 (1972); J. C. Polanyi, J. J. Sloan, and J. Wanner, *Chem. Phys.* **13**, 1 (1976).
- ⁶⁹M. A. Wickamaaratchi, D. W. Setser, B. Hildebrandt, B. Korbitzer, and H. Heydtman, *Chem. Phys.* **84**, 105 (1984).
- ⁷⁰D. G. Truhlar and B. C. Garrett, *Annu. Rev. Phys. Chem.* **35**, 159 (1984).
- ⁷¹A. Kupperman, *J. Phys. Chem.* **83**, 12 (1979).
- ⁷²D. G. Truhlar, B. C. Garrett, P. G. Hipes, and A. Kupperman, *J. Chem. Phys.* **81**, 3542 (1984); B. C. Garrett, D. G. Truhlar, R. S. Grev, and A. W. Magnuson, *J. Phys. Chem.* **84**, 1730 (1980); **87**, 4554(E) (1983); R. T. Skodje, D. G. Truhlar, and B. C. Garrett, *J. Chem. Phys.* **77**, 5955 (1982).
- ⁷³G. G. Lynch, D. G. Truhlar, and B. C. Garrett, *J. Chem. Phys.* **90**, 3102 (1989).
- ⁷⁴P. Pechukas, in Ref. 22.
- ⁷⁵H. Furue and P. D. Pacey, *J. Phys. Chem.* **90**, 397 (1986).
- ⁷⁶M. H. Mok and J. C. Polanyi, *J. Chem. Phys.* **51**, 1451 (1969).
- ⁷⁷L. M. Loewenstein and J. G. Anderson, *J. Phys. Chem.* **91**, 2993 (1987).
- ⁷⁸T. Takayanagi, N. Masaki, K. Nakamura, M. Okamoto, S. Sato, and G. Schatz, *J. Chem. Phys.* **86**, 6133 (1987); T. Takayanagi, K. Nakamura, and S. Sato, *ibid.* **90**, 1641 (1989).
- ⁷⁹D. Clary, *J. Chem. Soc. Faraday Trans. 2* **83**, 139 (1987).
- ⁸⁰T. Su and M. T. Bowers, in *Gas Phase Ion Chemistry*, (Academic, New York, 1979), Vol. 1, Chap. 3.
- ⁸¹R. B. Boodaghians, I. W. Hall, and R. P. Wagne, *J. Chem. Soc. Faraday Trans. 2* **82**, 529 (1987).
- ⁸²J. W. Hepburn, D. Klimek, K. Liu, J. C. Polanyi, and S. C. Wallace, *J. Chem. Phys.* **69**, 4311 (1978).
- ⁸³P. Baybutt, F. W. Bobrowicz, L. R. Kahn, and D. G. Truhlar, *J. Chem. Phys.* **68**, 4809 (1978).
- ⁸⁴D. C. Clary and J. N. L. Connor, *J. Phys. Chem.* **88**, 2758 (1984); J. Manz, R. Meyer, E. Pollak, and J. Roemelt, *Chem. Phys. Lett.* **93**, 184 (1982).
- ⁸⁵D. M. Garner, D. G. Fleming, D. J. Arseneau, M. Senba, and R. J. Mikula, *J. Chem. Phys.* (submitted); P. W. Percival, J. C. Brodovitch, S. K. Leung, D. Yu, R. F. Kiefl, D. M. Garner, D. J. Arseneau, D. G. Fleming, A. C. Gonzalez, J. R. Kempton, M. Senba, K. Venkateswaran, and S. F. J. Cox, *Chem. Phys. Lett.* (in press).
- ⁸⁶K. Lorenz, H. Gg. Wagner, and R. Zellner, *Ber. Bunsenges Phys. Chem.* **83**, 556 (1979).